BARD Final Report IS-4931-16C

The role of FLS3 and BSK830 in pattern-triggered immunity in tomato

Sessa, G. Tel Aviv University
Martin, G.B. Boyce Thompson Institute

Project award year: 2016
Three year research project

Abstract
Pattern-recognition receptors (PRRs) located on the plant cell surface initiate immune responses by perceiving conserved pathogen molecules known as pathogen-associated molecular patterns (PAMPs). PRRs typically function in multiprotein complexes that include transmembrane and cytoplasmic kinases and contribute to the initiation and signaling of pattern-triggered immunity (PTI). An important challenge is to identify molecular components of PRR complexes and downstream signaling pathways, and to understand the molecular mechanisms that mediate their function. In research activities supported by BARD-4931, we studied the role of the FLAGELLIN SENSING 3 (FLS3) PRR in the response of tomato leaves to flagellin-derived PAMPs and PTI. In addition, we investigated molecular properties of the tomato brassinosteroid signaling kinase 830 (BSK830) that physically interacts with FLS3 and is a candidate for acting in the FLS3 signaling pathway. Our investigation refers to the proposal original objectives that were to: 1) Investigate the role of FLS3 and its interacting proteins in PTI; 2) Investigate the role of BSK830 in PTI; 3) Examine molecular and phosphorylation dynamics of the FLS3-BSK830 interaction; 4) Examine the possible interaction of FLS3 and BSK830 with *Pst* and *Xcv* effectors.
We used CRISPR/Cas9 techniques to develop plants carrying single or combined mutations in the *FLS3* gene and in the paralogs *FLS2.1* and *FLS2.2* genes, which encode the receptor FLAGELLIN SENSING2 (FLS2), and analyzed their function in PTI. Domain swapping analysis of the FLS2 and FLS3 receptors revealed domains of the proteins responsible for PAMP detection and for the different ROS response initiated by flgII-28/FLS3 as compared to flg22/FLS2. In addition, *in vitro* kinase assays and point mutations analysis identified FLS2 and FLS3 domains required for kinase activity and ATP binding. In research activities on tomato BSK830, we found that it interacts with PRRs and with the co-receptor SERK3A and PAMP treatment affects part of these interactions. CRISPR/Cas9 *bsk830* mutant plants displayed enhanced pathogen susceptibility and reduced ROS production upon PAMP treatment. In addition, BSK830 interacted with 8 *Xanthomonas* type III secreted effectors. Follow up analysis revealed that among these effectors XopAE is part of an operon, is translocated into plant cells, and displays E3 ubiquitin ligase activity. Our investigation was also extended to other Arabidopsis and tomato BSK family members. Arabidopsis BSK5 localized to the plant cell periphery, interacted with receptor-like kinases, and it was phosphorylated *in vitro* by the PEPR1 and EFR PRRs. *bsk5* mutant plants displayed enhanced susceptibility to pathogens and were impaired in several, but not all, PAMP-induced responses. Conversely, BSK5 overexpression conferred enhanced disease resistance and caused stronger PTI responses. Genetic complementation suggested that proper localization, kinase activity, and phosphorylation by PRRs are critical for BSK5 function. BSK7 and BSK8 specifically interacted with the FLS2 PRR, their respective mutant plants were more susceptible to *B. cinerea* and displayed reduced flg22-induced responses. The tomato BSK Mai1 was found to interact with the M3Kα MAPKKK, which is involved in activation of cell death associated with effector-triggered immunity. Silencing of *Mai1* in *N. benthamiana* plants compromised cell death induced by a specific class of immune receptors. In addition, co-expression of Mai1 and M3Kα in leaves enhanced MAPK phosphorylation and cell death, suggesting that Mai1 acts as a molecular link between pathogen recognition and MAPK signaling. Finally, We identified the PP2C phosphatase Pic1 that acts as a negative regulator of PTI by interacting with and dephosphorylating the receptor-like cytoplasmic kinase Pti1, which is a positive regulator of plant immunity. The results of this investigation shed new light on the molecular characteristics and interactions of components of the immune system of crop plants providing new knowledge and tools for development of novel strategies for disease control.

Summary Sheet

Publication Summary

PubType	IS only	Joint	US only
Abstract - Poster	2	1	0
Abstract - Presentation	0	1	0
Reviewed	3	1	3
Submitted	0	1	0

Training Summary

Trainee Type	Last Name	First Name	Institution	Country
Postdoctoral Fellow	Majhi	Bharat	TAU	Israel
Ph.D. Student	Popov	Georgy	TAU	Israel
M.Sc. Student	Sobol	Guy	TAU	Israel
Postdoctoral Fellow	Roberts	Robyn	BTI	USA
Postdoctoral Fellow	Hind	Sarah	BTI	USA
Ph.D. Student	Sobol	Guy	Tel Aviv University	Israel

Contribution of collaboration

The achievements described in this report are the result of an active and synergistic collaboration between the Israeli and the American laboratories. Between the two labs there was a constant exchange of resources and expertise during the entire course of the project. CRISPR/Cas9 techniques were used at BTI to generate tomato plants mutated in the *FLS3*, *FLS2.1*, *FLS2.2*, *BSK830* genes. Phenotypic analysis of the *FLS3*, *FLS2.1* and *FLS2.2* mutant plants was performed at BTI, while *BSK830* mutant plants were transferred to the Israeli group and their PTI responses were characterized at TAU. For testing the interaction of the FLS3, FLS2.1 and BTI9 PRRs with *Xanthomonas* type III effectors, constructs were prepared at BTI and assays performed at TAU. Studies on Arabidopsis BSK5, BSK7 and BSK8 were carried out at TAU. Mai5 functional studies were carried out at BTI, while determination of Mai5 subcellular localization was performed at TAU. The Pic1 phosphatase was identified and biochemically characterized at BTI and PTI-associated Pic1 family members were identified at TAU. The PIs reviewed progress and future research activities, and outlined a renewal of the BARD grant during a visit of Prof. Sessa to BTI (May 2019) and a visit of Prof. Martin at TAU (September 2019). The two groups were frequently in touch by Email and skype video calls.

Major activities and achievements of this research were as follows:

1. Structure-function analysis of FLS3 (Hind et al., 2016 and 2017; Appendix 1). We used CRISPR/Cas9 to develop a tomato line with a mutation in the *FLAGELLIN SENSING3* (*FLS3*) gene and in both of the paralogs (*FLS2.1* and *FLS2.2*), which encode the receptor FLAGELLIN SENSING2 (FLS2). We also generated a tomato line mutated only for the two *FLS2* genes or for *FLS3* alone, and for *FLS2.1* alone. These lines are being used for rigorous testing of the relative importance of these three PRR genes in PTI. Domain swapping analysis of the FLS2 and FLS3 receptors demonstrated that the surface exposed LRR domain was sufficient for FLS3 detection of flgII-28, and that the transmembrane region was linked to the more extensive, sustained ROS response initiated by flgII-28/FLS3 as compared to flg22/FLS2. In addition, *in vitro* kinase assays and point mutations in the FLS2 and FLS3 catalytic domains revealed that the inner juxtamembrane domain is required for kinase activity and that the two proteins have similar structural requirements for ATP binding, but not for kinase activity.

2. Functional characterization of BSK family members (Majhi et al., 2019; Majhi and Sessa, 2019; Roberts et al., 2019; Appendix 2). We first focused on BSK830 and then extended our analysis to Arabidopsis BSK5, BSK7 and BSK8, and tomato BSK Mai1. BSK830 interacted with various tomato PRRs and with the co-receptor SERK3A (BAK1 homolog). The BSK830-FLS3 interaction in plant cells was reduced by flgII-28 treatment. We generated CRISPR/Cas9 *bsk830* mutant plants that displayed enhanced susceptibility to the fungus *Botrytis cinerea*, reduced ROS production upon pathogen-associated molecular pattern (PAMP) treatment, but normal MAPK activation. BSK5 localized to the plant cell periphery, interacted with multiple receptor-like kinases, and it was phosphorylated *in vitro* by the PEPR1 and EFR PRRs. *bsk5* mutants displayed enhanced susceptibility to the bacterium *Pseudomonas syringae* and to *B. cinerea* and were impaired in several, but not all, PAMP-induced immune responses. Conversely, BSK5 overexpression conferred enhanced disease resistance and caused stronger PTI responses. Genetic complementation suggested that localization to the cell periphery, kinase activity, and phosphorylation by PRRs are critical for BSK5 function. These findings demonstrate that BSK5 plays a key role in PTI by acting downstream of multiple immune receptors. BSK7 and BSK8 specifically interacted with the FLS2 PRR, their respective mutant plants were more susceptible to *B. cinerea* and *P. syringae*. In addition, consistent with a role in PTI signaling, *bsk7, bsk8,* and

bsk7bsk8 mutant plants treated with the PAMP flg22 displayed reduced accumulation of reactive oxygen species, callose deposition at the cell wall, and expression of the defense-related gene *PR1* compared to wild-type plants. Conversely, in both mutants, flg22-induced MAPK activation was unaltered. Together, these results suggest that BSK7 and BSK8 play roles in PTI downstream of FLS2. We identified the tomato BSK Mai1 as an interactor of the M3Kα MAPKKK, which is involved in activation of cell death associated with effector-triggered immunity. Silencing of *Mai1* in *N. benthamiana* plants increased susceptibility to *P. syringae* and compromised cell death induced by nucleotide-binding leucine-rich repeat (NLR) immune receptors of the coiled-coiled, but not of the TIR type. Cell death was restored by expression of a synthetic *Mai1* gene that resists silencing. In addition, co-expression of Mai1 and M3Kα in leaves enhanced MAPK phosphorylation and accelerated cell death, suggesting that Mai1 acts as a molecular link between pathogen recognition and MAPK signaling.

3. Examination of the interaction of FLS3 and BSK830 with *Xanthomonas euvesicatoria* (*Xe*) type III-secreted effectors (T3Es) (Popov et al., 2018). We tested the interaction of 35 *Xe* T3Es with the kinase domains of FLS3, FLS2.1 and BTI9 PRRs in *N. benthamiana* plants. None of the effectors interacted with any of the tested PRRs, while 8 T3Es interacted with BSK830. Among them, follow up analysis of XopAE from *Xe* strain 85-10 revealed that this effector is part of an operon, is translocated into plant cells through the type III secretion system, and translocation is dependent on its upstream ORF, *hpaF*. Homology modeling predicted that XopAE contains an E3 ligase XL box domain at the C terminus, and *in vitro* assays demonstrated that this domain displays monoubiquitination activity. Remarkably, the XL box was essential for XopAE to inhibit PAMP-induced gene expression in Arabidopsis protoplasts.

4. Identification of the PP2C phosphatase Pic1 as a negative regulator of PTI (Giska and Martin, 2019). We found that the PTI-inhibiting PP2C phosphatase (Pic1) interacts with and dephosphorylates the receptor-like cytoplasmic kinase Pti1b, which is a positive regulator of plant immune responses. An *in vitro* pull-down assay and *in vivo* split-luciferase complementation assay verified this interaction. Pti1b was found to autophosphorylate on threonine-233 and this phosphorylation was abolished in the presence of Pic1. An arginine-to-cysteine substitution at position 240 in the Arabidopsis MARIS kinase was previously reported

to convert it into a constitutive-active form. The analogous substitution in Pti1b made it resistant to Pic1 phosphatase activity, although it still interacted with Pic1. Treatment of *N. benthamiana* leaves with the PAMP flg22 induced threonine phosphorylation of Pti1b. Expression of Pic1, but not a phosphatase-inactive variant of this protein, in *N. benthamiana* leaves greatly reduced ROS production in response to treatment with the PAMPs flg22 or csp22. The results indicate that Pic1 acts as a negative regulator by dephosphorylating the Pti1b kinase, thereby interfering with its ability to activate plant immune responses. Finally, we found evidence that 13 PP2C phosphatase-encoding genes, including *Pic1*, are induced or suppressed during PTI activation and 8 of them significantly inhibit PAMP-induced ROS production when expressed in *N. benthamiana* plants.

Benefits to Agriculture

The results of our investigation contribute to the understanding of PTI mechanisms and will allow them to be manipulated by both molecular breeding and genetic engineering to produce plants with enhanced natural defense against disease. Moreover, because it is now apparent that all plants (both monocots and dicots) appear to use fundamentally similar resistance mechanisms our research might become relevant to many economically important plant species and to the control of diverse pathogens.

Changes to the original research plan

Preliminary experiments showed a physical interaction in yeast and *in planta* between FLS3 and BSK830. Based on these data, we hypothesized that FLS3 activates BSK830 by phosphorylation. However, because during the first year of research we did not detect phosphorylation of BSK830 by FLS3, we were not able to investigate phosphorylation dynamics of the FLS3-BSK830 interaction (objective 3). Instead, we expanded our investigation to the functional analysis of additional BSK family members in PTI or ETI signaling. These included tomato Mai5, which is involved in ETI-associated cell death, and Arabidopsis BSK5, BSK7 and BSK8, which play a role in PTI downstream of PRR receptors. In addition, we investigated the role in plant immunity of the PP2C phosphatase Pic1 that acts as a negative regulator of PTI by interacting with and dephosphorylating the receptor-like cytoplasmic kinase Pti1, which is a positive regulator of PTI.

Publications for Project IS-4931-16C

Status	Type	Authors	Title	Journal	Vol:pg Year	Coun
Published	Reviewed	*Hind S.R., J.S. Hoki, J.A. Baccile, P.C. Boyle, F.C. Schroeder and G.B. Martin*	Detecting the interaction of peptide ligands with plant membrane receptors	***Curr. Protoc. Plant Biol.***	2 : 240-269 2017	US only
Published	Reviewed	*Giska F., and G.B. Martin*	PP2C phosphatase Pic1 negatively regulates the phosphorylation status of Pti1b kinase, a regulator of flagellin-triggered immunity in tomato	***Biochem. J.***	476 : 1621-1635 2019	US only
Published	Abstract - Poster	*Majhi B.B., S. Sreeramulu and G.Sessa*	The receptor-like cytoplasmic kinase BSK5 associates with immune receptors and is required for PTI	***MPMI Conference (Glasgow, Scotland)***	: 2019	IS only
Published	Abstract - Poster	*Sobol G., B.B. Majhi and G. Sessa*	Arabidopsis thaliana BSK7 and BSK8 are involved in PTI signaling	***Conference COST CA16107 EuroXanth (Halle, Germany)***	: 2018	IS only
Submitted	Abstract - Poster	*Sobol G., B.B. Majhi, N. Zhang, HM Roberts, G.B. Martin*	The tomato receptor-like cytoplasmic kinase BSK830 associates with immune receptors and plays a role in PTI	***Plant Biotic Stresses & Resistance Mechanisms IV (Vienna, Austria)***	: 2020	Joint
Published	Abstract - Poster	*Sobol G., B.B. Majhi, N. Zhang, HM Roberts, G.B. Martin*	The role of the tomato receptor-like cytoplasmic kinase BSK830 in PTI signaling	***MPMI Conference (Glasgow, Scotland)***	: 2019	Joint
Published	Abstract - Presentation	*Majhi, B.B., Sreeramulu, S., Popov, G., Hind, S.H., Roberts, R., Martin, G.B. and Sessa, G.*	BSK5 is a component of PTI signaling, and its tomato homolog BSK830 interacts with multiple Xanthomonas euvesicatoria effectors	***Conference COST CA16107 EuroXanth (Coimbra, Portugal)***	: 2017	Joint
Published	Reviewed	*Hind, S.R., S.R. Strickler, P.C. Boyle, D.M. Dunham, Z. Bao, I.M. O'Doherty, J.A. Baccile, J.S. Hoki, E.G. Viox, C.R. Clarke, B.A. Vinatzer, F.C. Schroeder and G.B. Martin*	Tomato receptor FLAGELLIN-SENSING 3 binds flgII-28 and activates the plant immune system	***Nature Plants***	2 : 16128 2016	US only
Published	Reviewed	*Hind, S.R., R. Roberts, K.F. Pedley, B.A. Diner, M.J. Szarzanowicz, D. Luciano-Rosario, B.B. Majhi, G. Popov, G. Sessa, C.-S. Oh and G. B.*	Mai1 protein acts between host recognition of pathogen effectors and mitogen-activated protein kinase signaling	***Mol. Plant-Microbe Interact.***	32 : 1496-1507 2019	Joint

		Martin				
Published	Reviewed	*Popov, G., B. B. Majhi, and G. Sessa*	Effector gene xopAE of Xanthomonas euvesicatoria 85-10 is part of an operon and encodes an E3 ubiquitin ligase	***J. Bacteriol.***	200 : e00104-18 2018	IS only
Published	Reviewed	*Majhi, B. B., S. Sreeramulu, and G. Sessa*	BRASSINOSTEROID-SIGNALING KINASE5 associates with immune receptors and Is required for immune responses	***Plant Physiol.***	180 : 1166-1184 2019	IS only
Published	Reviewed	*Majhi B.B. and G. Sessa*	Overexpression of BSK5 in Arabidopsis thaliana provides enhanced disease resistance	***Plant Signal Behav.***	14 : e1637665 2019	IS only

Appendix 1. Functional characterization of tomato FLS3.

1. Generation of FL3, FLS2.1 and FLS2.2 mutant lines. We used CRISPR/Cas9 to develop a tomato line with a mutation in the *FLAGELLIN SENSING3* (*FLS3*) gene and in both of the paralogs (*FLS2.1* and *FLS2.2*), which encode the receptor FLAGELLIN SENSING2 (FLS2). We also generated a tomato line mutated only for the two *FLS2* genes or for *FLS3* alone, and for *FLS2.1* alone. These lines are being used for rigorous testing of the relative importance of these three PRR genes in PTI. We confirmed all of the knockout phenotypes using the PAMPs flg22 and flgII-28 in reactive oxygen species (ROS) assays. To determine the contributions of FLS3 to PTI, we conducted bacterial population assays by vacuum infiltrating the plants and comparing the populations of *Pst* strains DC3000 Δ*avrPto/*Δ*avrPtoB* and DC3000 Δ*avrPto/*Δ*avrPtoB/fliC* (*fliC* encodes flagellin). Our data suggests the FLS2 and FLS3 are the major (or only) determinants of flagellin-derived PTI, and that FLS3 and FLS2 contribute equally to PTI.

2. Structure-function analysis of FLS3. We observed that the generation of ROS is initiated faster and sustained over a much longer time period for the flgII-28/FLS3 response as compared with the flg22/FLS2 response (Fig. 1). This observation suggests that these two PRRs use different molecular mechanisms to activate early signaling events like ROS production. To investigate possible mechanistic differences between FLS3 and FLS2, we developed chimeric constructs that have different combinations of the LRR domain, transmembrane region, and the kinase domain from the two flagellin-sensing proteins. We then transiently expressed these chimeric PRR proteins in *N. benthamiana* leaves and measured the ROS response to flg22 and flgII-28. These experiments revealed that the LRR domain of FLS3 is sufficient for detection of the flgII-28 peptide and consequent ROS production (Fig. 2). In addition, whether the ROS response is FLS2-like or FLS3-like (faster and more sustained) depends on the origin of the transmembrane region (Fig. 2).

It has been reported previously that a consensus sequence in subdomain I is important in positioning ATP in protein kinases (Schwessinger et al. 2011, PLoS Genetics **7**:e1002046), and that a G879S mutation in the consensus sequence from GxGxxG results in a predicted 50-fold decrease in kinase activity of FLS2. We cloned the kinase domains (KD) and the kinase domains plus the inner juxtamembrane domains (JM+KD) of FLS2 and FLS3 and tested their kinase activities. In our experimental conditions, both FLS3 and FLS2 from tomato have strong kinase activity compared to a Pto kinase control, and that the inner juxtamembrane domain is required for this activity (Fig. 3). To see if mutations in subdomain

I influence kinase activity, we mutated FLS3 and FLS2 JM+KD proteins to match their protein counterparts (FLS2 or FLS3, respectively). We found that mutating G858S in FLS3 of subdomain I to match FLS2 caused a loss of FLS3 autophosphorylation. However, the S881G mutation in FLS2 to match FLS3 caused no loss of function, suggesting that FLS3 and FLS2 have different mechanisms for their kinase activation. We also made a mutation in FLS3 that causes a reduced ROS response to see if the ROS response is linked to kinase activity (T1011P). However, this mutation caused no loss in autophosphorylation of FLS3, suggesting that the reduced ROS response is not related to kinase activation. Finally, we made substitutions in the ATP binding sites of both proteins that causes a loss-of-function in FLS3 and FLS2 (K877Q and K900Q, respectively). We are currently creating additional mutations in the inner juxtamembrane and kinase domains to test the requirement for different conserved residues in subdomain I and other domains, and developing chimeric constructs that swap the inner juxtamembrane domains between FLS2 and FLS3 to see if specificity is required for activity.

Figures Appendix 1

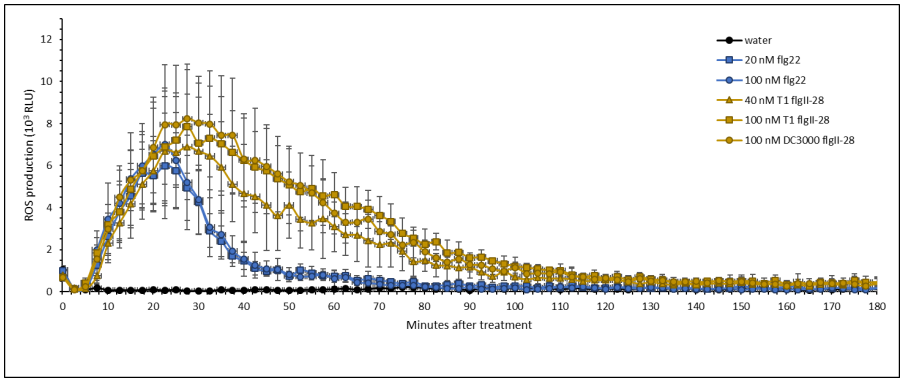

Figure 1. The initiation and duration of reactive oxygen species production by flg22/FLS2 and flgII-28/FLS3 region differ. Tomato leaf discs were exposed to different amounts of flg22 or flgII-28 (present in *Pst* strain T1 or DC3000) and ROS production was measured over a time course using a chemiluminescence assay.

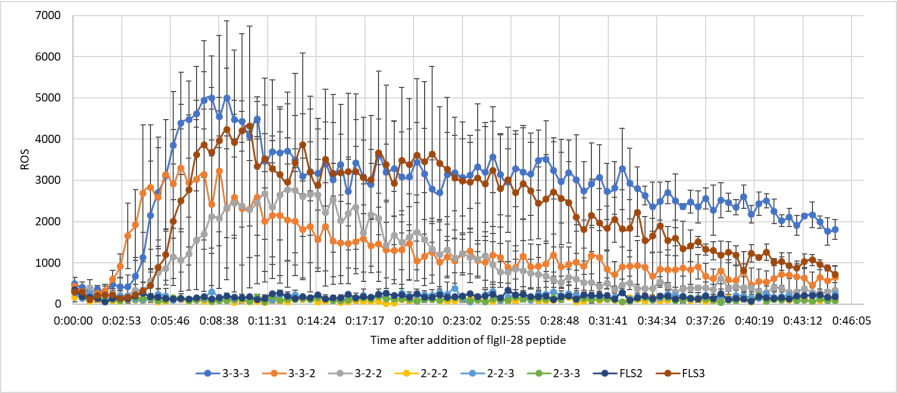

Figure 2. The FLS3 LRR domain is sufficient for detection of flgII-28 and the transmembrane domain affects the initiation and duration of the response to flgII-28. ROS output from *N. benthamiana* leaves expressing chimeric proteins in response to flgII-28 (100 nM). In the legend, the first number denotes the origin of the LRR domain (FLS3 = 3 and FLS2 = 2), the second number denotes the origin of the transmembrane region, and the last number denotes the origin of kinase domain.

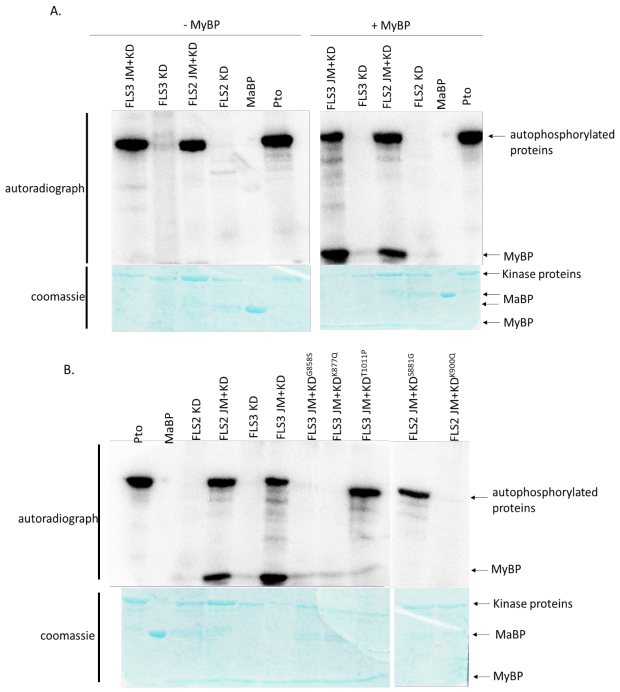

Figure 3. FLS3 requires the inner juxtamembrane domain for kinase activity. A) FLS3 and FLS2 kinase domain only (KD) or kinase domain plus the inner juxtamembrane domain (JM+KD) proteins tagged with maltose binding protein (MaBP) were tested in *in vitro* kinase assays with or without myelin basic protein (MyBP) as a substrate. B) Mutations in FLS2 or FLS3 were made in the conserved subdomain I region to match their counterpart in FLS2 (G585S) or FLS3 (S881G). A mutation in FLS3 known to reduce ROS response (Hind et al. 2017) was made to see if this mutation is linked to kinase activity (T1011P). Mutations in the ATP binding site were made as loss-of-function mutants (K877Q and K900Q). In A and B, Pto was used as a positive control and MaBP was used as a negative control. Coomassie stained gels were used to verify equal loading.

Appendix 2. Functional characterization of tomato BSK830

1. BSK830 interacts with multiple PRRs and the PRR co-receptor SERK3A. To start investigating if the seven tomato BSK family members play a role in plant immunity, BSKs were individually used as bait and the kinase domain of three PRRs (FLS2, FLS3, and Bti9) as preys and their physical interactions were monitored in yeast. Solyc12g099830 (hereafter BSK830) interacted with all three PRRs, while the other BSK family members did not show any interaction (Fig. 1A). Next, a split luciferase complementation assay (SLCA) was employed to validate *in planta* the interactions observed in yeast. In this experiment, the three PRRs were fused to the C-terminal half of the luciferase protein (C-LUC) and co-expressed via *Agrobacterium* in *N. benthamiana* leaves with each of the BSK family members fused to the N-terminal half of the luciferase protein (N-LUC). As negative controls, C-LUC-PRRs were co-expressed with the N-LUC empty vector and N-LUC-BSKs were co-expressed with the C-LUC empty vector. Protein interactions were quantified by measurement of emitted luminescence in the tested leaves at 48 h after agro-infiltration. Co-expression of BSK830 or its closest homolog Solyc11g064890 (hereafter BSK890) with FLS2, FLS3, and Bti9, resulted in emission of luminescence that is significantly higher than that obtained in the negative controls (Fig. 1B). A similar experiment was performed to check the interaction of BSK830 and BSK890 with the PRR co-receptors SERK3A and SERK3B. Both BSK830 and BSK890 interacted with SERK3A, but not with SERK3B (Fig. 1C). Together, these results indicate that BSK830 and BSK890 physically interact with multiple PRRs and the PRR co-receptor SERK3A.

2. BSK830 dynamically interacts with FLS3, and is not phosphorylated by FLS2, FLS3, and SERK3A *in vitro*. To test the hypothesis that PAMP perception modulates the PRR-BSK830 interaction, we employed SLCA assays. BSK830 and FLS3 were co-expressed by agro-infiltration in *N. benthamiana.* After 48 h, infiltrated leaves were treated with water or flgII-28 (100 nM). As shown in Fig. 2A, the FLS3-BSK830 interaction was reduced upon flgII-28 elicitation suggesting that BSK830 is released following activation. Next, to assess whether FLS3 activates BSK830 by phosphorylation, we tested the requirement of FLS3 kinase activity for the dissociation of the FLS3-BSK830 complex. In this experiment we employed a form of FLS3 ($FLS3_{K877Q}$) mutated in the conserved lysine of the kinase ATP binding site and monitored dynamics of its interaction in the presence or absence of flgII-28. $FLS3_{K877Q}$ interacted with BSK830 similarly to the wild-type FLS3 in the absence flgII-28 (Fig. 2B). However, the $FLS3_{K877Q}$-BSK830 interaction was not affected by flgII-28 treatment as

opposed to the FLS3-BSK830 interaction (Fig. 2B). These results imply that kinase activity of FLS3 is necessary for the release of the FLS3-BSK830 complex in response to flgII-28. To test whether BSK830 is a substrate of RLK phosphorylation, we tested whether the cytoplasmic domain of FLS2 ($FLS2_{CD}$), FLS3 ($FLS3_{CD}$), or SERKA ($SERK3A_{CD}$) phosphorylate BSK830. BSK890 was used to assess phosphorylation specificity, whereas the phosphorylation of *At*BSK5 by *At*BRI1 was used as positive control. MBP-BSK830, MBP-BSK890, MBP-$FLS2_{CD}$, MBP-$FLS3_{CD}$, and MBP-$SERK3A_{CD}$ fusion proteins were expressed in *E. coli*, purified, and incubated in the presence of [γ-^{32}P]ATP. Reactions were fractionated by SDS-PAGE, transferred onto a PVDF membrane and exposed to autoradiography. $FLS2_{CD}$, $FLS3_{CD}$, and $SERK3A_{CD}$ were able to autophosphorylate, but did not phosphorylate BSK830 or BSK890 (Fig. 3). Both BSK830 and BSK890 did not show autophosphorylation activity (Fig 2, C-E) supporting the notion that BSKs are pseudokinases.

3. BSK830 localizes to the cell periphery through an N-myristoylation site. To investigate its subcellular localization, BSK830 in the wild-type form or carrying a mutation in a putative myristoylation site (G2A), was fused upstream to the yellow fluorescent protein (YFP). The fusion proteins were transiently expressed in *N. benthamiana* leaves by agro-infiltration and their localization was monitored by confocal microscopy. A cyan fluorescent protein (CFP) which localizes to both the cytoplasm and nucleus was used as control. Localization was examined by monitoring of fluorescence 36 h post agro-infiltration. BSK830-YFP localized exclusively to the cell periphery, while the localization pattern of $BSK830_{G2A}$-YFP was similar to that of CFP (Fig. 3). This suggests that BSK830 localizes to the cell periphery, likely to the plasma membrane by N-terminal myristoylation. To examine whether BSK830 changes its localization upon PAMP elicitation, leaves expressing BSK830-YFP were treated with water or flg22 (100 nM) and its localization was monitored 30 min later. No change in the BSK830 localization pattern was observed (Fig. 3), suggesting that BSK830 is not released from the cell periphery upon PTI activation.

4. Generation of *bsk830* mutant and *BSK830-YFP* overexpression lines. To investigate the role of BSK830 in PTI, we generated *bsk830* mutant and overexpression plants in the tomato line Hawaii 7981. We developed two individual homozygous lines mutated in *BSK830* using CRISPR/Cas9 (Fig. 4A, 4B) and 5 lines overexpressing the BSK830-YFP fusion protein(Fig. 4C, 4D). The mutants were allowed to segregate until the desired homozygous genotype was achieved at the T2 generation. The area flanking the sgRNA was PCR-amplified, sequenced and compared with the wild-type (Fig. 4A). Sequence comparison revealed a 4 bp deletion

(*bsk830-1*) or a 135 bp deletion (*bsk830-2*). Both mutant lines displayed a stunted growth phenotype compared to wild-type plants. Protein expression of BSK830-YFP in the transgenic lines was validated by Western blot with anti-GFP antibodies (Fig. 4C) and by monitoring of YFP fluorescence using a confocal microscope. The observed fluorescence was localized to the cell periphery, similarly to what was observed in *N. benthamiana* (Fig. 3).

5. *bsk830* mutants display reduced ROS production and susceptibility to *B. cinerea*. To investigate the role of BSK830 in plant immunity, we tested susceptibility of two *bsk830* mutant plants to the necrotrophic fungal pathogen *Botrytis cinerea*. Leaves of wild-type, *bsk830-1*, and *bsk830-2* plants were inoculated with *B. cinerea* by placement of a 4 mm agar disc covered with mycelium. Inoculated leaves were monitored for development of lesions whose diameter was measured at 3 dpi. Lesions were significantly larger in leaves of *bsk830* mutants than in wild-type plants (Fig. 5A). This result suggests that BSK830 is involved in tomato resistance against *B. cinerea*. To test the involvement of BSK830 in the activation of PTI responses, wild-type and *bsk830* mutant plants were treated with flg22 or flgII-28 and monitored for production of ROS and MAPK activation. *fls2.1/fls2.2* and *fls3* mutants were used as controls in these experiments. *bsk830* mutant plants revealed a reduced accumulation of reactive oxygen species upon treatment with the flg22 and flgII-28 peptides (Fig. 5B). However, MAPK activation by flg22 and flgII-28 remained unaltered in these plants (Fig. 5C). The *fls2.1/fls2.2* and *fls3* mutants were unable to respond to flg22 and flgII-28, respectively, did not accumulate ROS, and showed lower MAPK phosphorylation levels. These results suggest that BSK830 plays a role in PTI-associated ROS production, but not in MAPK activation.

6. Seven type III *Xe* effectors interact with BSK830. As a first step to test the hypothesis that type III effectors target BSK830 and other components of tomato PTI signaling, we used SLCA in *N. benthamiana* plants to test the interaction of BSK830, FLS2, FLS3, and Bti9 with 35 *Xe* effectors. None of the effectors interacted with any of the tested PRRs, while seven effectors interacted with BSK830 (Fig. 6). These results suggest that BSK830 may be a target of *Xe* type III effectors.

Figures Appendix 2

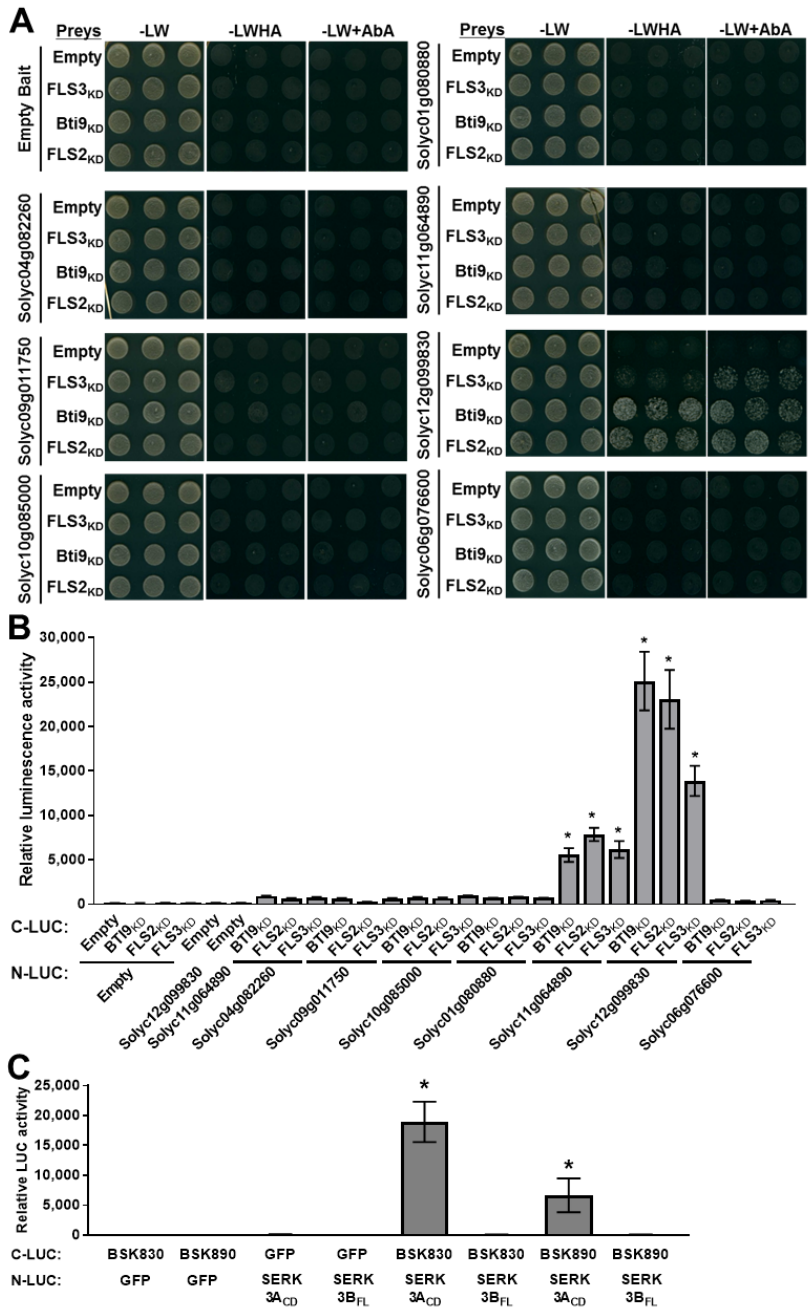

Figure 1. Interaction of tomato RLKs FLS2, FLS3, Bti9, SERK3A, and SERK3B with BSK family members. (A) Yeast cells expressing the each BSK family member fused to the GAL4 DNA-binding domain (bait), and the kinase domain of the indicated PRRs fused to the GAL4 DNA-activation domain (prey) were grown on synthetically defined (SD) medium lacking Leu and Trp (-LW), SD –LW lacking His, and Ade (-LWHA), or SD –LW supplemented with with Aureobasidin A (-LW+AbA). Empty vectors (Empty) were used as negative controls. (B, C) The indicated proteins were fused to either C-LUC or N-LUC and co-expressed in *N. benthamiana* leaves by agro-infiltration. Luciferase activity was quantified by measuring relative luminescence units (RLU) at 48 h after agro-infiltration. The data represents means ± SE of luminescence values measured from five leaf discs sampled from three different plants. Asterisks indicate statistically significant difference (Student's *t*-test, *P* value < 0.05) relative to N-LUC-Empty or N-LUC-GFP.

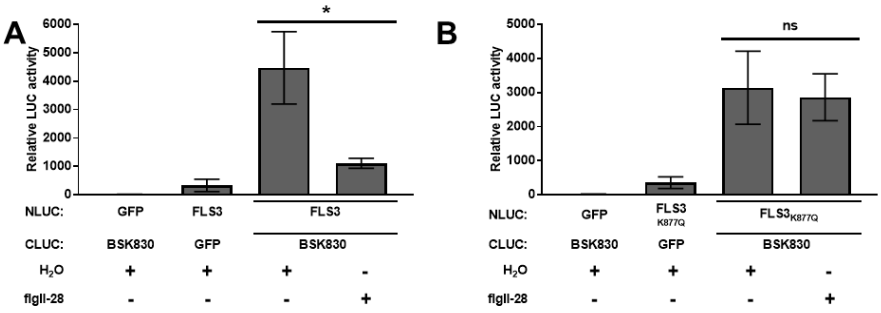

Figure 2. Effect of PAMP treatment on the FLS3-BSK830 interaction. (A, B) The indicated proteins were fused to either C-LUC or N-LUC and co-expressed in *N. benthamiana* leaves by agro-infiltration. After 48 h, the infiltrated areas were treated with water or flgII-28 (100 nM), and luciferase activity was quantified 30 min later by measuring relative luminescence units (RLU). The data represents means ± SE of luminescence values measured from five leaf discs sampled from three different plants.

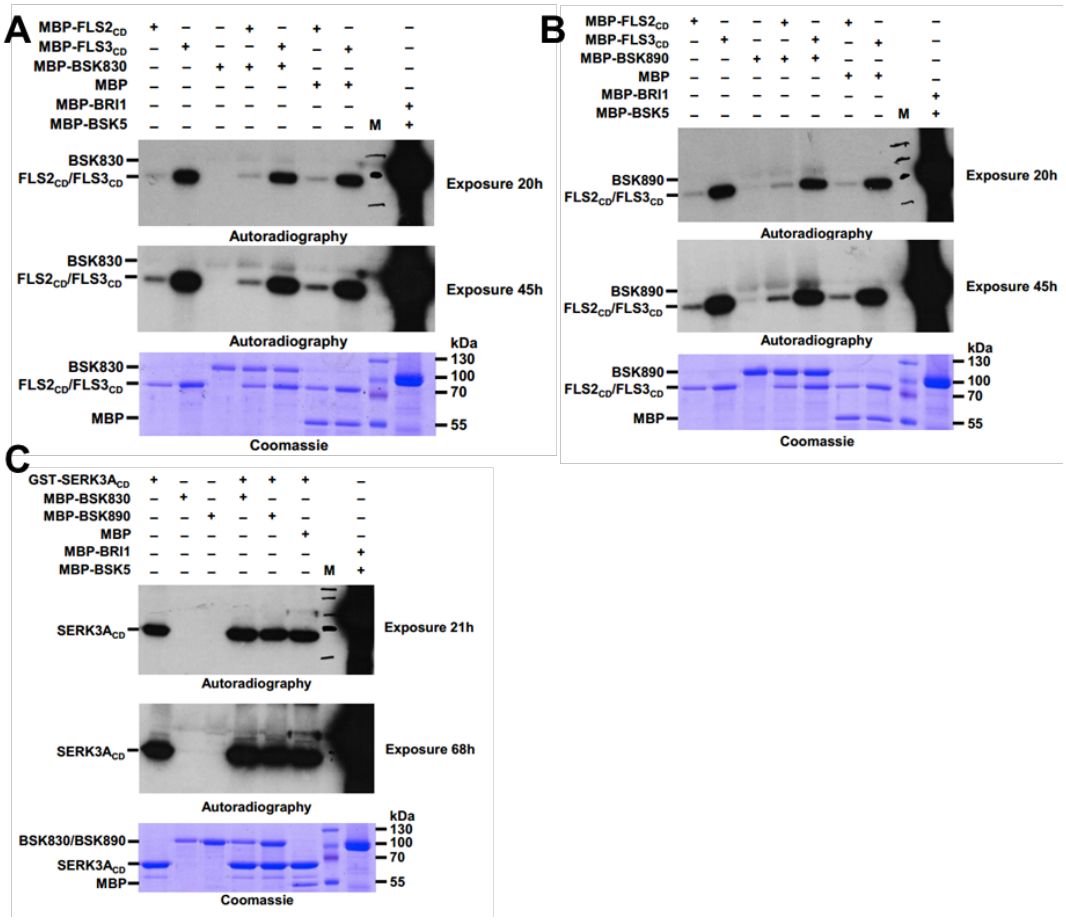

Figure 3. BSK830 is not phosphorylated *in vitro* by FLS2, FLS3, and SERK3A. Phosphorylation of MBP-BSK830, and MBP-BSK890 by MBP-FLS2$_{CD}$, MBP-FLS3$_{CD}$ (A, B) and MBP-SERK3A$_{CD}$ (C) was assayed *in vitro* in the presence of [γ-^{32}P]ATP. Phosphorylation of MBP-BSK5 by MBP-BRI1 was used as the positive control. Proteins were fractionated by SDS-PAGE and either transferred to a PVDF membrane and exposed to autoradiography, or stained with Coomassie brilliant blue.

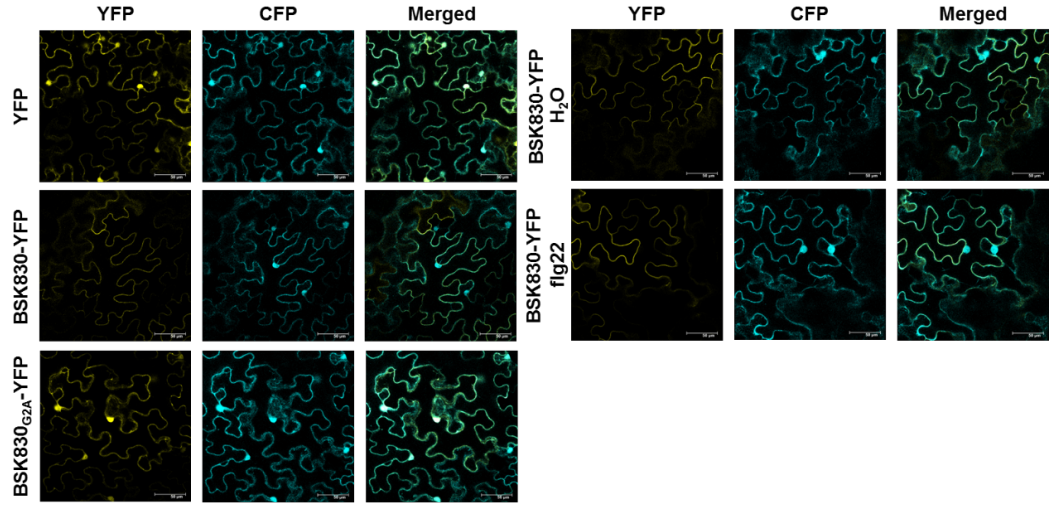

Figure 3. BSK830 localizes to the cell periphery through myristoylation in *N. benthamiana*. The BSK830-YFP and BSK830$_{G2A}$-YFP fusion proteins were co-expressed with the cyan fluorescent protein (CFP) in *N. benthamiana* leaves via *Agrobacterium*. 36 h after agro-infiltration, leaves co-expressing BSK830-YFP and CFP were infiltrated with either water, 100 nM of flg22, or untreated. Fluorescence was monitored in epidermal cells by confocal microscopy 36 h after infiltration or 30 min after flg22 treatment. YFP, CFP, and merged fluorescence images are shown. Scale bars represent 50 µM.

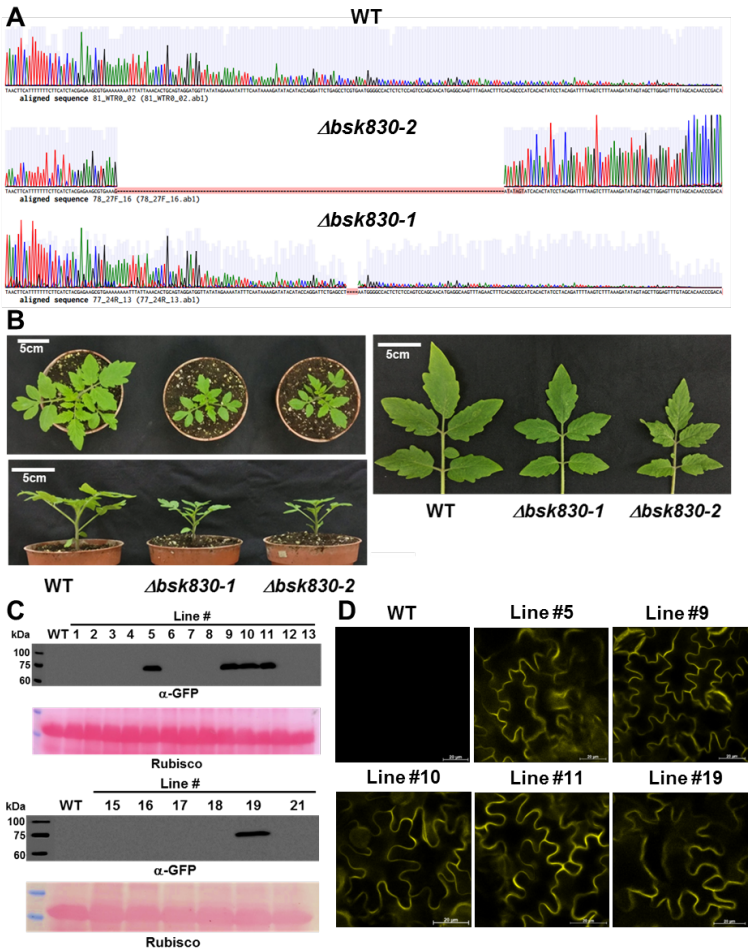

Figure 4. Generation of *bsk830* mutants and *BSK830-YFP* overexpression lines. (A) Multiple sequence alignment of the *BSK830* gene locus in wild-type, *bsk830-1*, and *bsk830-2* plants. (B) Morphological differences between 4 weeks-old wild-type and *bsk830* mutant plants. (C) Validation of BSK830-YFP fusion proteins expression in the obtained transgenic lines by a Western blot developed with anti-GFP antibodies. (D) Validation of BSK830-YFP fusion proteins expression in the transgenic lines by monitoring fluorescence in tomato epidermal cells by confocal microscopy. YFP fluorescence images are shown. Scale bars represent 20 µM.

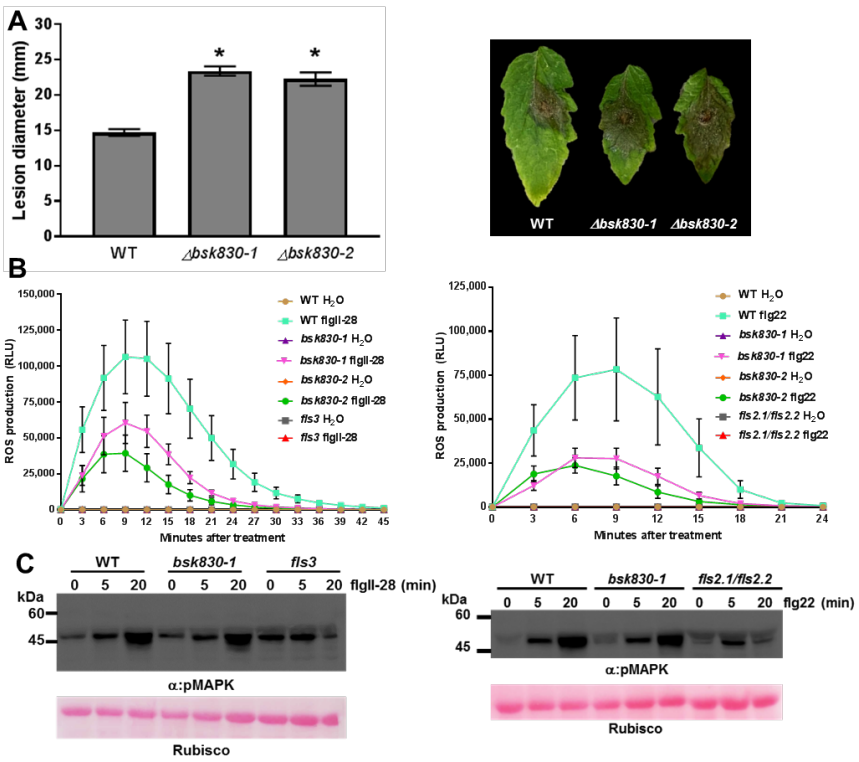

Figure 5. BSK830 contributes to immunity against *B. cinerea* and plays a role in ROS production. (A) Susceptibility to *B. cinerea*. Leaves of wild-type (WT), *bsk830-1*, and *bsk830-2* were inoculated with *B. cinerea* by placement of a 4 mm agar disc covered with mycelium. The lesion diameter was measured at 3 dpi (left panel) and representative leaves were photographed (right panel). Data are means ± SE of at least 10 lesions from three different plants. Asterisks indicate a significant difference (Student's *t* test, *P* value < 0.05) compared to wild-type plants. (B) ROS production. Leaf discs from plants were treated with either water, 1 µM flg22, or 1 µM flgII-28, and incubated with luminol and horseradish peroxidase. Luminescence was measured as relative luminescence unit (RLU) in 3 minute intervals. Data are means ± SE of 5 leaf discs from 3 different plants. (C) MAPK activation. Leaf discs were floated overnight in water and treated with flg22, or flgII-28 (1 µM), or water. Samples were harvested at 0, 5 and 20 min after treatment and analyzed by Western blot with anti-pMAPK antibody (α:pMAPK). Ponceau S staining of Rubisco is shown as a loading control.

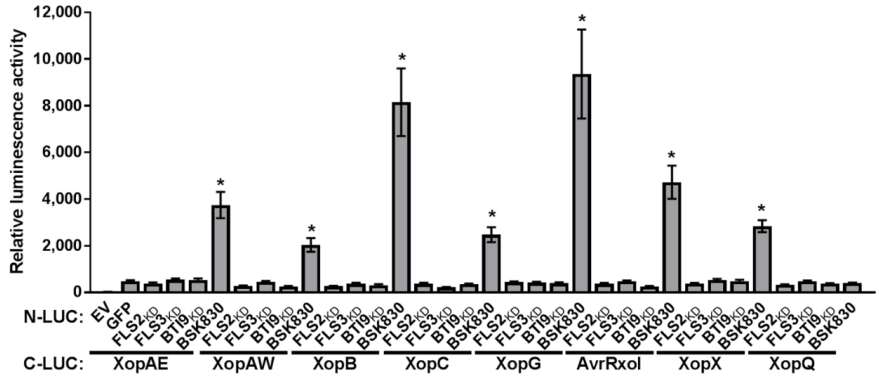

Figure 6. Seven *Xe* type III effectors interact with BSK830 by SLCA in *N. benthamiana*. The indicated proteins were fused to either C-LUC or N-LUC and co-expressed in *N. benthamiana* leaves by agro-infiltration. Luciferase activity was quantified by measurement of relative luminescence units (RLU) at 36 h after agro-infiltration. The data represent mean ± SE of luminescence values measured from five leaf discs sampled from three different plants. Asterisks indicate statistically significant difference (Student's *t* test, *P* value < 0.05) relative to N-LUC-Empty.